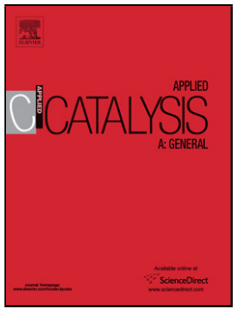

Title: Efficient hydrodesulfurization catalysts based on Keggin polyoxometalates

Author: Jocelyn North Olivia Poole Abdullah Alotaibi Hossein Bayahia Elena F. Kozhevnikova Ali Alsalme M. Rafiq H. Siddiqui Ivan V. Kozhevnikov

PII: S0926-860X(15)30178-2
DOI: http://dx.doi.org/doi:10.1016/j.apcata.2015.10.001
Reference: APCATA 15577

To appear in: *Applied Catalysis A: General*

Received date: 24-8-2015
Revised date: 23-9-2015
Accepted date: 1-10-2015

Please cite this article as: Jocelyn North, Olivia Poole, Abdullah Alotaibi, Hossein Bayahia, Elena F.Kozhevnikova, Ali Alsalme, M.Rafiq H.Siddiqui, Ivan V.Kozhevnikov, Efficient hydrodesulfurization catalysts based on Keggin polyoxometalates, Applied Catalysis A, General http://dx.doi.org/10.1016/j.apcata.2015.10.001

Efficient hydrodesulfurization catalysts based on Keggin polyoxometalates

Jocelyn North[1], Olivia Poole[1], Abdullah Alotaibi[1], Hossein Bayahia[1], Elena F. Kozhevnikova[1], Ali Alsalme[2], M. Rafiq H. Siddiqui[2], Ivan V. Kozhevnikov[1*]

[1]*Department of Chemistry, University of Liverpool, Liverpool L69 7ZD, United Kingdom*

[2]*Department of Chemistry, King Saud University, P.O. Box 2455, Riyadh, Kingdom of Saudi Arabia*

[*] Corresponding author. Tel.: +44(0)1517942938
E-mail address: kozhev@liverpool.ac.uk (I. V. Kozhevnikov)

Graphical abstract

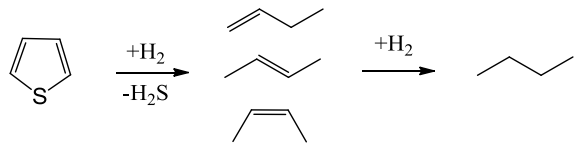

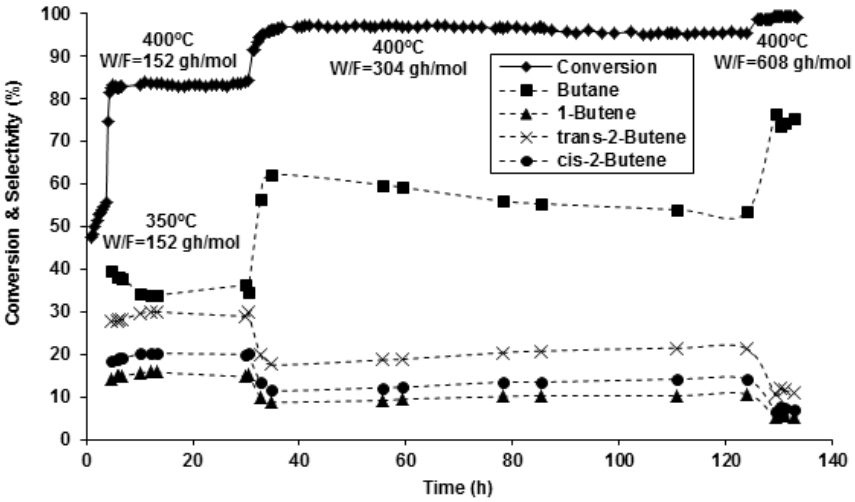

Highlights

- HDS pre-catalysts prepared via polyoxometalate (POM) route retain the POM structure and acidity.
- The structure and acidity lost upon sulfidation to form HDS active phase(s).
- HDS activity increases in the series of supports: SiO_2<TiO_2<γ-Al_2O_3.
- POM-based CoMo catalyst more active and selective in thiophene HDS than industrial counterpart.

Abstract

Bulk and supported hydrodesulfurization catalysts based on Mo and W and containing Co or Ni as promoters and phosphorus as a modifier are prepared through the polyoxometalate route using Keggin type phosphomolybdates and phosphotungstates and tested in the HDS of thiophene at 350-400 ^{o}C and 1 bar pressure. The corresponding oxidic pre-catalysts retain intact Keggin structure of the parent polyoxometalates and possess Brønsted and Lewis acidity. In the course of sulfidation, the oxidic pre-catalysts transform into an active sulfidic phase with the loss of Keggin structure and catalyst acidity. Catalyst activity increases in the order of supports: SiO_2 < TiO_2 < γ-Al_2O_3. CoMoP/γ-Al_2O_3 catalyst prepared through the polyoxometalate route shows higher HDS activity and butene selectivity than industrial catalyst of comparable composition. The results indicate that polyoxometalate catalyst preparation route can be considered a performance enhancement methodology for HDS catalysis.

Key words: desulfurization, thiophene, heterogeneous catalysis, polyoxometalate, molybdenum, cobalt.

1. Introduction

Hydrodesulfurization (HDS) driven by ever stringent environmental legislation is one of the most important processes of the petroleum industry. It removes sulfur from oil fractions by catalytic hydrotreatment to upgrade the quality of fuels [1,2]. Present day HDS technology largely employs sulfided Co(Ni)Mo/γ-Al_2O_3 catalysts [1-3]. These catalysts, although durable, are not sufficiently active and selective to achieve the required very low sulfur content in transportation fuels. Consequently, research into improvement of HDS catalysts continues all over the world. Recent developments include new methods of preparation of Co(Ni)Mo catalysts such as chemical vapor deposition improving the dispersion of active phases [4], addition of phosphorus [4] and citric acid [5], new active phases for HDS catalysts, e.g., noble metals [6], transition metal carbides [7], nitrides [8] and phosphides [9,10].

The Co(Ni)Mo/Al_2O_3 HDS catalysts are obtained by in-situ sulfidation of an oxidic precursor (pre-catalyst), which is usually prepared by impregnation of γ-alumina support with appropriate Mo and Co(Ni) compounds from aqueous solution, most typically using ammonium heptamolybdate and adding Co(II) or Ni(II) nitrate as a promoter, often with addition of phosphoric acid as a modifier [1-3]. Depending on the pH and P and Mo concentrations, such impregnation solutions contain P-Mo heteropoly anions such as $P_2Mo_5O_{23}^{6-}$, $PMo_9O_{31}(OH)_3^{6-}$, $PMo_{11}O_{39}^{7-}$, $PMo_{12}O_{40}^{3-}$ and $P_2Mo_{18}O_{62}^{6-}$ [2]. On the other hand, heteropoly compounds, especially molybdophosphates incorporating Co(II) and/or Ni(II) promoters as counter cations or addenda atoms, can be used directly for the preparation of oxidic precursors for HDS catalysts [11-23]. In the past decades, heteropoly compounds, also known as polyoxometalates (POM) [24], have

attracted much interest as catalysts of various reactions and as such found application in several large-scale industrial processes [25-27]. Various types of heteropoly compounds have been used for the preparation of HDS pre-catalysts, the common Keggin type heteropoly compounds comprising heteropoly anions of the composition $[XM_{12}O_{40}]^{n-}$ (M = Mo^{6+}, W^{6+}; X = P^{5+}, Si^{4+}) most frequently applied. Catalyst preparation methodology through the polyoxometalate route has important advantages such as (i) incorporation of all the elements required for HDS catalyst within heteropoly compound thus allowing the preparation of oxidic precursor in a single impregnation step, (ii) close interaction between the key elements in the pre-catalyst and sulfided catalyst and (iii) extraneous counter ions can be excluded from the impregnation solution to reduce waste [16,17].

In this work, which follows up our recent study on polyoxometalate $NiMo/SiO_2$ HDS catalysts [23], we prepared bulk and supported Co and Ni phosphomolybdate and phosphotungstate catalysts via the POM route from Co(II) and Ni(II) salts of phosphomolybdic $H_3[PMo_{12}O_{40}]$ and phosphotungstic $H_3[PW_{12}O_{40}]$ heteropoly acids (HPA) and tested for their activity in the HDS of thiophene, which is relevant to the hydrotreating of FCC naphtha [1,2]. Our aim was to investigate the effect of POM composition and catalyst support on the catalytic activity, the role of Brønsted and Lewis acidity of the pre-catalyst and to follow the evolution of pre-catalyst in the course of HDS reaction. It is demonstrated that $CoMo/Al_2O_3$ catalyst prepared through the POM route has the potential of reducing hydrogen consumption in HDS process and the loss of high octane alkenes in the final gasoline pool. Therefore, the POM catalyst preparation route can be considered a performance enhancement methodology for HDS catalysis.

2. Materials and methods

2.1. Chemicals and materials

Phosphomolybdic and phosphotungstic acid hydrates ($H_3[PMo_{12}O_{40}]\cdot 12H_2O$ and $H_3[PW_{12}O_{40}]\cdot 28H_2O$), $Ni(NO_3)_2\cdot 6H_2O$, $Co(NO_3)_2\cdot 6H_2O$ and thiophene (99%) were from Sigma-Aldrich. Catalyst supports Aerosil 300 silica (S_{BET} = 300 m^2g^{-1}), P25 titania (anatase/rutile = 3:1, S_{BET} = 51 m^2g^{-1}) and Aluminiumoxid C γ-alumina (S_{BET} = 120 m^2g^{-1}) were from Degussa.

2.2. Preparation of HDS pre-catalysts

Bulk Ni(II) and Co(II) salts of $H_3[PMo_{12}O_{40}]$ and $H_3[PW_{12}O_{40}]$ with M(II)/HPA molar ratios of 1:1 and 1.5:1 (i.e., M(II)/Mo(VI) or M(II)/W(VI) ratio of 1:12 and 1:8) were prepared by dissolving the HPA in a minimum amount of deionized water at room temperature followed by addition of the required amount of the corresponding metal nitrate ($Co(NO_3)_2$ or $Ni(NO_3)_2$) with stirring. Excess water was distilled off using a rotary evaporator and the resulting residue oven dried at 100 ^oC overnight. The solids were calcined in air at 350 ^oC for 2 h with a heating rate of 10 ^oC $min^{-1}$and finally ground into a powder of 45-180 μm particle size.

Supported $H_3[PMo_{12}O_{40}]$ and $H_3[PW_{12}O_{40}]$ pre-catalysts with 30 wt% HPA loading based on anhydrous HPA were prepared by wet impregnation of support (γ-Al_2O_3, SiO_2 or TiO_2) with an aqueous solution of HPA at room temperature with stirring for 2 h. Solid residues were isolated by rotary evaporation, oven dried at 100 ^oC and air calcined at 350 ^oC for 2 h at a heating rate of 10 ^oC min^{-1}. The pre-catalysts were then ground into a

powder with a particle size of 45-180 μm. γ-Al_2O_3-supported Ni(II) and Co(II) phosphomolybdate and phosphotungstate pre-catalysts with M(II)/HPA molar ratios of 1:1 and 1.5:1 and 30 wt% POM loading were prepared similarly by impregnation of γ-Al_2O_3 with HPA and $Ni(NO_3)_2$ or $Co(NO_3)_2$ in required quantities from aqueous solution. The slurry was stirred for 2 h at room temperature followed by rotary evaporation to remove water. The residue was dried overnight at 100 ^oC and air calcined at 350 ^oC for 2 h resulting in lightly colored powders, which were ground into 45-180 μm particle size.

Industrial $CoMo/Al_2O_3$ pre-catalyst (ICI Catalyst 41-6, Co/Mo = 0.62 mol/mol), containing CoO (4.0%), MoO_3 (12.0%), SiO_2 (1.0%) and γ-Al_2O_3 (balance) [3], was crushed and sieved to a powder with a particle size of 45-180 μm. It had a surface area of 220 m^2g^{-1} and a pore volume of 0.6 cm^3g^{-1} [3]. For comparison with the industrial ICI 41-6 catalyst, $15\%Co_{1.5}[PMo_{12}O_{40}]/Al_2O_3$ pre-catalyst containing similar Mo loading (13% MoO_3) but a lower Co/Mo molar ratio of 0.125 was prepared by grinding $30\%Co_{1.5}[PMo_{12}O_{40}]/Al_2O_3$ with equal quantity of γ-Al_2O_3 support. The powder was pressed into a pellet then crushed to a 45-180 μm catalyst powder.

2.3. Techniques

Catalyst surface area, pore volume and pore size were determined on a Micromeritics ASAP 2010 instrument by measuring nitrogen adsorption at -196 ^oC. Before measurement the catalysts were pre-treated at 240 ^oC in vacuum. Powder X-ray diffractograms were collected on a PANalytical Xpert diffractometer using Cu Kα radiation (λ = 0.1542 nm). ICP-AES analysis of sulfur was carried out on a Spectro Ciros emission spectrometer. Fourier transform infrared (FTIR) spectra of pre-catalysts and

spent catalysts were recorded on a Nicolet Nexus FTIR spectrometer using powdered catalyst mixtures with KBr. In FTIR spectra of γ-Al_2O_3-supported catalysts, the absorption of support was subtracted using a γ-Al_2O_3-KBr mixture as the background. DRIFT (diffuse reflectance infrared Fourier transform) spectra of adsorbed pyridine were taken on the same spectrometer. Catalyst samples were ground with KBr (1-10 wt% in KBr) and pre-treated at 150 $^oC/10^{-3}$ kPa for 1 h. The samples were then exposed to pyridine vapor at room temperature for 1 h, followed by pumping out at 150 $^oC/10^{-3}$ kPa for 1 h to remove physisorbed pyridine. The DRIFT spectra of adsorbed pyridine were recorded at room temperature at a 4 cm^{-1} resolution. Temperature programmed reduction (H_2-TPR) of catalysts was carried out on a Micromeritics TPD/TPR 2900 apparatus equipped with a thermal conductivity detector. Catalyst samples (20-30 mg) were heated up to 950 ^oC at a rate of 10 ^oC min^{-1} in a H_2-N_2 (5:95) gas flow (60 mL min^{-1}).

2.4. Catalyst testing

The HDS of thiophene was carried out in flowing H_2 at 350-400 ^oC under atmospheric pressure in a down-flow quartz fixed-bed reactor (9 mm i.d.) with online GC analysis (Varian 3800 instrument with a 30 m × 0.25 mm × 0.5 μm HP-INNOWAX capillary column and a flame ionization detector) (Supplementary material, Fig. S1). For more accurate offline GC analysis of C_1-C_4 hydrocarbon products, a 60 m x 0.32 mm GS-GasPro capillary column was used, which allowed for complete separation of these hydrocarbons. The temperature in the reactor was controlled by a Eurotherm controller using a thermocouple placed at the top of the catalyst bed. Thiophene was fed by passing hydrogen flow controlled by a Brooks mass flow controller through a stainless steel

saturator which held liquid thiophene at 0 °C to keep the chosen thiophene partial pressure of 2.63 kPa in hydrogen flow [28]. The reactor was packed with 0.2-0.4 g of pre-catalyst powder of 45–180 μm particle size. The gas feed entered the reactor at the top at a flow rate of 10-20 mL min^{-1} (space time W/F = 152-608 g h mol^{-1}, where W (g) is the catalyst weight and F (mol h^{-1}) is the molar flow rate of thiophene). Prior to reaction monitoring, the pre-catalysts were sulfided in situ in the feed flow containing thiophene (2.63 kPa) in H_2 for 1 h at the reaction temperature. The downstream flow was analyzed by the on-line GC to continuously monitor thiophene conversion. Product selectivity was determined at selected times on stream by offline GC analysis using the GS-GasPro capillary column. The selectivity was defined as the percentage of thiophene converted into a particular product and quoted in mol. %. The mean absolute percentage error in conversion and selectivity was ≤ 5% and the carbon balance was maintained within 95%.

3. Results and discussion

3.1. Pre-catalyst characterization

Bulk HPA and M(II)-HPA (M = Co, Ni) pre-catalysts prepared had a very low surface area (2.3-5.7 m^2g^{-1}) and pore volume (0.004-0.012 cm^3g^{-1}), which is typical of these compounds [25-27]; their pore diameter was in the range of 58-114 Å (Table S1). The M(II)-HPA pre-catalysts with the sub-stoichiometric M(II)/HPA molar ratio of 1:1 can be viewed as the partially substituted heteropoly salts $M^{II}H[PMo_{12}O_{40}]$ and $M^{II}H[PW_{12}O_{40}]$. For the stoichiometric M(II)/HPA ratio of 1.5:1, the pre-catalysts could be attributed to neutral salts $M^{II}_{1.5}[PMo_{12}O_{40}]$ and $M^{II}_{1.5}[PW_{12}O_{40}]$, although HPA salts

prepared to be neutral often contain protons due to incomplete substitution and Keggin ion degradation [27]. It should be noted that Ni(II) and Co(II) nitrates decompose to form metal oxides upon calcination above 300 ^{o}C: $M(NO_3)_2 \rightarrow MO + 2NO_2 + O_2$ [29]. From powder X-ray diffraction (XRD), bulk $H_3[PMo_{12}O_{40}]$ and $H_3[PW_{12}O_{40}]$ calcined at 350 ^{o}C were crystalline materials with close packed cubic structure. Bulk metal salts of $H_3[PW_{12}O_{40}]$ were crystalline too, whereas the salts of $H_3[PMo_{12}O_{40}]$ were amorphous as exemplified for Co(II) salts in Fig. 1.

Supported HPA and M(II)-HPA pre-catalysts (30 wt% loading) prepared through Keggin POMs were mesoporous materials with a BET surface area of 29-172 m^2g^{-1}, 0.14-0.86 cm^3g^{-1} pore volume and 119-249 Å pore diameter depending on support (γ-Al_2O_3, SiO_2 or TiO_2) (Table S2). The $Co_{1.5}[PMo_{12}O_{40}]/Al_2O_3$ pre-catalyst, which showed the highest activity among the catalysts studied (see below), had a surface area of 69 m^2g^{-1}, 0.27 cm^3g^{-1} pore volume and 157 Å pore diameter. For this catalyst, nitrogen adsorption isotherm and pore size distribution are shown in Fig. S2 and Fig. S3.

$H_3[PMo_{12}O_{40}]$ exhibited a crystal phase on SiO_2 and Al_2O_3, but was amorphous on TiO_2 (Fig. S4). $H_3[PW_{12}O_{40}]$ was crystalline on SiO_2 and TiO_2, but amorphous on Al_2O_3 (Fig. S4). Co(II) and Ni(II) salts of $H_3[PMo_{12}O_{40}]$ were crystalline on Al_2O_3 (Fig. 2), whereas the salts of $H_3[PW_{12}O_{40}]$ did not show POM crystal phase on Al_2O_3 (Fig. S5).

Regardless of crystallinity, the Keggin primary structure of PMo and PW heteropoly anions remained intact in all these materials, bulk and supported, as demonstrated by infrared spectroscopy. Fig. 3 and Fig. 4 show the DRIFT spectra of bulk $Co_{1.5}[PMo_{12}O_{40}]$ and $NiH[PW_{12}O_{40}]$ pre-catalysts (powdered with KBr), which match perfectly the literature spectra of $H_3[PMo_{12}O_{40}]$ and $H_3[PW_{12}O_{40}]$ and their salts [30]. Fig.

5 shows the DRIFT spectrum of $Co_{1.5}[PMo_{12}O_{40}]/Al_2O_3$ pre-catalyst, with the strong absorption band of alumina at 900 cm^{-1} largely subtracted. It also matches quite well the literature spectra of bulk $H_3[PMo_{12}O_{40}]$ and its salts (cm^{-1}): 1062-1068 (P-O), 954-963 (Mo=O), 869-880 (Mo-O-Mo corner-sharing) and 785-805 (Mo-O-Mo edge-sharing) [30]. In the spectrum of $Co_{1.5}[PMo_{12}O_{40}]/Al_2O_3$, the weak Mo-O-Mo bands at 865 and 803 cm^{-1} are partly obscured by the γ-Al_2O_3 band at 900 cm^{-1}.

M(II)-HPA pre-catalysts possess Brønsted and Lewis acidity owing to the presence of heteropoly acid protons and M(II). These materials showed the characteristic peaks of Brønsted (~1540 cm^{-1}) and Lewis (~1450 cm^{-1}) acid sites in their DRIFT spectra of adsorbed pyridine, together with the band at 1490 cm^{-1} attributed to both types of acid sites [31] as exemplified for bulk $NiH[PMo_{12}O_{40}]$ in Fig. 6. This acidity, however, was lost during the HDS reaction as a result of catalyst sulfidation (see below).

Fig. 7 shows the H_2-TPR (temperature programmed reduction) of $H_3[PMo_{12}O_{40}]/Al_2O_3$ and $Co_{1.5}[PMo_{12}O_{40}]/Al_2O_3$ pre-catalysts. Both exhibit two reduction peaks at about 550 and 800 ^oC. The Keggin structure of HPMo would probably collapse to form MoO_3 and P_2O_5 before the reduction took place. These peaks can be attributed to reduction of Mo(VI) to Mo(IV). As Mo(VI) is in large excess over Co(II) in the $Co_{1.5}[PMo_{12}O_{40}]/Al_2O_3$ pre-catalyst, reduction of Co(II) is probably masked by the Mo peaks. Similar H_2-TPR results have been reported previously for Ni(II)-$[PMo_{12}O_{40}]/SiO_2$ [23] and non-promoted $HPMo/TiO_2$ [17].

3.2. Catalyst performance in HDS of thiophene

3.2.1. Bulk catalysts

Bulk M(II)-HPA pre-catalysts have low surface areas and porosities (Table S1) and therefore could be expected to have low HDS activities. Nevertheless, it is interesting to test these catalysts because their evolution in the course of HDS reaction is easier to follow with spectroscopic techniques as compared to supported catalysts.

Table 1 shows the performance of the bulk HPA and M(II)-HPA catalysts in the HDS of thiophene at 400 ^{o}C and a space time W/F = 152 g h mol^{-1}. It is clearly seen that tungsten catalysts possessing more stable POM structure [27] are less active (<1% thiophene conversion) than more labile molybdenum catalysts (2-3.5% conversion). Ni-Mo catalysts show marginally higher activities than Co-Mo ones, the latter being practically equal in activity to the non-promoted $H_3[PMo_{12}O_{40}]$. The main reaction products include n-butane (10-21% selectivity) and n-butenes (1-butene, trans-2-butene and cis-2-butene) (30-59%), as represented by eq. (1). On top of that, significant amount of C_1-C_3 cracking by-products (25-60%) and a little of isobutane was also formed, which may be explained by strong acidity of the bulk HPA pre-catalysts (see above).

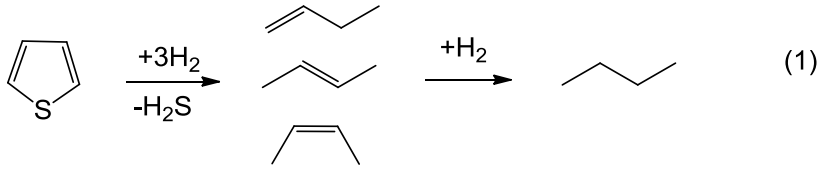

(1)

All bulk catalysts, initially lightly colored, turned black after reaction. This was also the case for supported M(II)-HPA catalysts (see below). The change of color indicates catalyst sulfidation. Indeed, from post-reaction characterization, sulfur content

in spent $Ni_{1.5}[PMo_{12}O_{40}]$ and $Co_{1.5}[PMo_{12}O_{40}]$ catalysts was found to be 7.5 and 4.5 wt%, which corresponds to 18 and 10% catalyst sulfidation, respectively, as estimated assuming formation of MoS_2 and NiS or CoS. This implies transformation of M(II)-$H_3[PMo_{12}O_{40}]$ pre-catalysts into active metal sulfide phases. A small amount of coke was also found in spent catalysts (0.32% carbon content in spent $Co_{1.5}[PMo_{12}O_{40}]$).

Amorphous bulk Co(II)-$H_3[PMo_{12}O_{40}]$ and Ni(II)-$H_3[PMo_{12}O_{40}]$ pre-catalysts remained amorphous after HDS reaction (Fig. 1). It was found that they lost their Keggin structure during the reaction as can be seen from Fig. 3, which shows the DRIFT spectra for $Co_{1.5}[PMo_{12}O_{40}]$ (pre-catalyst versus spent catalyst). In contrast, the more stable and less active M(II)-$H_3[PW_{12}O_{40}]$ catalysts retained the Keggin structure after reaction as clearly seen from the DRIFT spectra for $NiH[PW_{12}O_{40}]$ (Fig. 4). As to the M(II)-$H_3[PMo_{12}O_{40}]$ catalysts, not only their Keggin structure but also their acidity, both Brønsted and Lewis, was lost in the course of HDS reaction, as seen from the DRIFT spectra of adsorbed pyridine for the $NiH[PMo_{12}O_{40}]$ pre-catalyst and spent catalyst (Fig. 6).

The overall picture emerging from these results is that the M(II)-$H_3[PMo_{12}O_{40}]$ oxidic pre-catalysts with labile POM structure readily undergo sulfidation with the loss of Keggin structure and acidity to form an HDS active sulfidic phase. In contrast, the more stable M(II)-$H_3[PW_{12}O_{40}]$ pre-catalysts are rather resistant to sulfidation hence having difficulty to form active HDS catalysts, which results in their low catalytic activity.

3.2.2. Supported catalysts

Table 2 shows the HDS of thiophene over non-promoted supported HPA catalysts at 400 ^{o}C. These catalysts had considerably higher activities than their bulk counterparts, which can be attributed to higher HPA dispersion in supported catalysts. Again, for the reasons given above, Mo catalysts showed higher HDS activities in comparison to W catalysts. The type of support played an important role; the HDS activity (thiophene conversion) of Mo catalysts increased in the order of supports: SiO_2 < TiO_2 < γ-Al_2O_3, which is in agreement with previous reports [1,2]. This activity order does not correlate with support surface area (Table S2), but is in line with increasing HPA-support interaction in this series [27,32], which might increase dispersion of active species on the surface of support. It should be noted that the supported HPA catalysts were much more selective than the bulk ones, giving butane-butene product mixtures with only traces of C_1-C_3 cracking by-products (cf. results in Table 1 and Table 2). Therefore, as the alumina-supported Mo catalysts showed better HDS activities, our further studies were focused on these catalysts.

Table 3 shows the HDS of thiophene at 350-400 ^{o}C over γ-Al_2O_3-supported catalysts promoted by Co and Ni prepared through the POM route. It is evident that Mo catalysts are again much more active than their W counterparts. As expected, addition of Co and Ni promoters significantly increased thiophene conversion. The catalyst activity also increased with increasing the M(II)/HPA molar ratio. In all cases the catalyst activity predictably increased with increasing the temperature from 350 to 400 ^{o}C.

Among the catalysts studied, 30%$Co_{1.5}[PMo_{12}O_{40}]/Al_2O_3$ was found to be the most active one in the HDS of thiophene, closely followed by 30%$Ni_{1.5}[PMo_{12}O_{40}]/Al_2O_3$

(Table 3). The 30%$Co_{1.5}[PMo_{12}O_{40}]/Al_2O_3$ catalyst was tested for a longer time on stream (132 h in total) at different space times; the results are shown in Fig. 8. At 350 ºC and *W/F* = 152 g h mol^{-1}, thiophene conversion gradually increased with the time on stream from 47 to 55% in 4 h. This can be explained by increasing catalyst sulfidation to form an active sulfidic phase. At 400 ºC and the same space time, the sulfided catalyst performed with a steady conversion of 83%. A notable increase in butene selectivity occurred along the time on stream (from 38 to 47%) at the expense of n-butane formation. This may be explained by inhibition of catalyst hydrogenation activity due to coke formation. The conversion further scaled with the *W/F* to 96% at *W/F* = 304 g h mol^{-1} and 99% at 608 g h mol^{-1} without evidence of catalyst deactivation. The selectivity to n-butane increased with thiophene conversion at the expense of butenes reaching 75% at 99% conversion (Fig. 8). Only traces of C_1-C_3 cracking by-products were observed (Fig. S6), which can be explained by the loss of catalyst acidity upon sulfidation.

After reaction, the lightly colored 30%$Co_{1.5}[PMo_{12}O_{40}]/Al_2O_3$ pre-catalyst turned black, however its texture practically did not change (Table S2). Post-reaction characterization revealed only a small amount of coke in the spent catalyst (0.69 wt% carbon content). The sulfur content was found to be 8.2 wt%. This corresponds to 64% catalyst sulfidation assuming formation of MoS_2 and CoS and implies transformation of the pre-catalyst into an active metal sulfide phase on the alumina surface (hence the black color). Upon sulfidation, the Keggin structure of P-Mo polyoxometalate was completely destroyed as clearly seen from the DRIFT spectra of the pre-catalyst and spent catalyst (Fig. 5). Previously, non-promoted $H_3[PW_{12}O_{40}]$ has been found to lose its Keggin structure upon the HDS of dibenzothiophene as evidenced by ^{31}P MAS NMR [15].

No correlation was found between the activity of the M(II)-$H_3[PMo_{12}O_{40}]$ catalysts in the HDS of thiophene and the redox behavior of the corresponding pre-catalysts in H_2-TPR (Fig. 7). It is obvious that the HDS proceeds at much lower temperatures (350-400 ^oC) compared to the H_2-TPR (550–800 ^oC). This implies that sulfidation of these pre-catalysts to form catalytically active phases occurs at lower temperatures than their reduction with H_2. It should be noted, however, that the H_2-TPR was carried out under transient conditions. Slow isothermal catalyst reduction with H_2 may be possible at lower temperatures below 550 ^oC.

Thermodynamic analysis of reaction products provides further evidence about the HDS process. The equilibrium ratio of n-butene isomers has been found to be 1-butene/trans-2-butene/cis-2-butene = 1:1.8:1.2 at 400 ^oC and 1 bar [33]. This is close to the ratio obtained here with M(II)-$H_3[PMo_{12}O_{40}]$ catalysts (Table 3), which shows that the butenes produced were at equilibrium. On the other hand, hydrogenation of butenes to n-butane was far from equilibrium, with butane/butene molar ratios 2-3 orders of magnitude lower than the equilibrium values. This indicates that butene-to-butane hydrogenation was a slow process, and as a result, n-butane selectivity predictably increased with thiophene conversion.

For comparison with industrial oxide pre-catalyst CoMo/γ-Al_2O_3 (ICI Catalyst 41-6) with 12% MoO_3 content and a Co/Mo molar ratio of 0.62 [3], the 30%$Co_{1.5}[PMo_{12}O_{40}]/Al_2O_3$ pre-catalyst was diluted with γ-Al_2O_3 to 15%$Co_{1.5}[PMo_{12}O_{40}]/Al_2O_3$ with a similar MoO_3 content (13%) but a lower Co/Mo molar ratio of 0.125. This catalyst was tested at 400 ^oC to give 54% thiophene conversion with 77% total butene selectivity at W/F = 152 g h mol^{-1} and 74% conversion with 64% butene

selectivity at *W/F* = 304 g h mol^{-1} (Fig. 9, Table 3). The industrial catalyst ICI 41-6 under the same conditions gave 37% conversion with 74% butene selectivity at *W/F* = 152 g h mol^{-1} and 54% conversion with 62% butene selectivity at *W/F* = 304 g h mol^{-1} (Fig. 10, Table 3). The spent ICI 41-6 catalyst contained 0.26% of coke and its sulfidation was 65% based on the formation of MoS_2 and CoS, which is close to the sulfidation of the 30%$Co_{1.5}[PMo_{12}O_{40}]/Al_2O_3$ catalyst (see above). Both 15%$Co_{1.5}[PMo_{12}O_{40}]/Al_2O_3$ and ICI 41-6 catalysts showed a slight decrease in n-butane selectivity with the time on stream (Fig. 9 and 10) probably due to inhibition of their hydrogenation activity by coking, similar to that displayed in Fig. 8. In the latter case, however, this trend is more notable due to much longer time on stream.

Therefore, the $Co_{1.5}[PMo_{12}O_{40}]/Al_2O_3$ catalyst, despite its lower Co/Mo ratio, gave higher thiophene conversion compared to the industrial catalyst per equal catalyst weight. It also gave higher butene selectivity thus exhibiting lower hydrogenation activity compared to the industrial catalyst, which can be explained by the lower Co content. Overall, these results demonstrate that the $Co_{1.5}[PMo_{12}O_{40}]/Al_2O_3$ catalyst prepared through the POM route has enhanced HDS performance compared to the conventional industrial $CoMo/Al_2O_3$ catalyst. This can be attributed to close interaction between oxomolybdenum species with Co promoter and to the presence of phosphorus modifier in the $Co_{1.5}[PMo_{12}O_{40}]/Al_2O_3$ catalyst.

4. Conclusions

It has been demonstrated that the $Co_{1.5}[PMo_{12}O_{40}]/Al_2O_3$ catalyst (Co/Mo = 0.125 mol/mol) prepared through the POM route using Keggin type phosphomolybdate has high activity in the HDS of thiophene. Compared to the industrial $CoMo/Al_2O_3$ catalyst with similar Mo loading and a higher Co/Mo ratio of 0.62, the new catalyst shows higher thiophene conversion and higher butene selectivity. Therefore $Co_{1.5}[PMo_{12}O_{40}]/Al_2O_3$ catalyst has the potential of reducing hydrogen consumption in HDS process and the loss of high octane alkenes in the final gasoline pool. On the basis of these results, the POM catalyst preparation route is considered to be a performance enhancement methodology for HDS catalysis.

Acknowledgements

This research was partly funded by the National Plan for Science, Technology and Innovation (MAARIFAH), King Abdulaziz City for Science and Technology, Saudi Arabia, Award No. 11-NAN-1852-02. We thank Shaqra University, Shaqra, Saudi Arabia for PhD studentship (A. Alotaibi).

References

[1] I. V. Babich, J. A. Moulijn, *Fuel* 82 (2003) 607-31.

[2] R. Prins, in *Handbook of Heterogeneous Catalysis*, ed. G. Ertl, H. Knözinger, F. Schüth, J. Weitkamp, Vol. 6, Wiley-VCH, Weinheim, 2008, p. 2695-2718.

[3] P. J. H. Carnell, in *Catalyst Handbook*, ed. M. V. Twigg, Wolfe Publishing, London, 1989, p. 204-208.

[4] Y. Okamoto, *Catal. Today* 132 (2008) 9–17.

[5] N. Rinaldi, K. Usman, T. Al-Dalama, Y. Kubota, Okamoto, *Appl. Catal. A* 360 (2009) 130–136.

[6] A. Niquille-Röthlisberger, R. Prins, *Catal. Today* 123 (2007) 198–207.

[7] M. Lewandowski, A. Szyma´nska-Kolasa, P. Da Costa, C. Sayag, *Catal. Today* 119 (2007) 31–34.

[8] M. Nagai, *Appl. Catal. A* 322 (2007) 178–190.

[9] Y. Kanda, C. Temma, A. Sawada, M. Sugioka, Y. Uemichi, *Appl. Catal. A* 475 (2014) 410–419.

[10] R. Prins, M. E. Bussell, *Catal. Lett*. 142 (2012) 1413–1436.

[11] S. Damyanova, A. Spojakina, D. Shopov, *Appl. Catal*. 48 (1989) 177-186.

[12] A. M. Maitra, N. W. Cant, D. L. Trimm, *Appl. Catal*. 48 (1989) 187-197.

[13] A. Griboval, P. Blanchard, L. Gengembre, E. Payen, M. Fournier, J. L. Dubois, J. R. Bernard, *J. Catal*. 188 (1999) 102–110.

[14] C. I. Cabello, I. L. Botto, H. J. Thomas, *Appl. Catal. A* 197 (2000) 79-86.

[15] R. Shafi, M. R. H. Siddiqui, G. J. Hutchings, E. G. Derouane, I. V. Kozhenikov, *Appl. Catal. A* 204 (2000) 251-256.

[16] A. Griboval, P. Blanchard, E. Payen, M. Fournier, J. L. Dubois, J. R. Bernard, *Appl. Catal. A* 217 (2001) 173–183.

[17] E. Kraleva, A. Spojakina, K. Jiratova, L. Petrov, *Catal. Lett*. 112 (2006) 203-212.

[18] R. Palcheva, A. Spojakina, K. Jiratova, L. Kaluza, *Catal. Lett*. 137 (2010) 216-223.

[19] K. Ben Tayeb, C. Lamonier, C. Lancelot, M. Fournier, A. Bonduelle-Skrzypczak, F. Bertoncini, *Appl. Catal. B* 126 (2012) 55–63.

[20] P. A. Nikul'shin, A. V. Mozhaev, D. I. Ishutenko, P. P. Minaev, A. I. Lyashenko, A. A. Pimerzin, *Kinet. Catal*. 53 (2012) 620-631.

[21] F. J. Méndez, A. Llanos, M. Echeverría, R. Jáuregui, Y. Villasana, Y. Díaz, G. Liendo-Polanco, M. A. Ramos-García, T. Zoltan, J. L. Brito, *Fuel* 110 (2013) 249–258.

[22] B. Pawelec, R. Mariscal, J. L. G. Fierro, A. Greenwood, P. T. Vasudevan, *Appl. Catal. A* 206 (2001) 295–307.

[23] A. Alsalme, N. Alzaqri, A. Alsaleh, M. R. H. Siddiqui, A. Alotaibi, E. F. Kozhevnikova, I. V. Kozhevnikov, *Appl. Catal. B* 182 (2016) 102-108.

[24] M. T. Pope, *Heteropoly and Isopoly Oxometalates*, Springer, Berlin, 1983.

[25] T. Okuhara, N. Mizuno, M. Misono, *Adv. Catal*. 41 (1996) 113-252.

[26] I. V. Kozhevnikov, *Chem. Rev*. 98 (1998) 171-198.

[27] I. V. Kozhevnikov, *Catalysis by Polyoxometalates*, Wiley & Sons, Chichester, 2002.

[28] D. R. Stull, *Ind. Eng. Chem*. 39 (1947) 517-550.

[29] S. Yuvaraj, L. Fan-Yuan, C. Tsong-Huei, Y. Chuin-Tih, S. Yuvaraj, L. Fan-Yuan, C. Tsong-Huei and Y. Chuin-Tih, *J. Phys. Chem. B* 107 (2003) 1044-1047.

[30] C. Rocchiccioli-Deltcheff, M. Fournier, R. Franck, R. Thouvenot, *Inorg. Chem*. 22 (1983) 207-216.

[31] H. Knözinger, in *Handbook of Heterogeneous Catalysis*, ed. G. Ertl, H. Knözinger, F. Schüth, J. Weitkamp, Wiley-VCH, Weinheim, 2008, p. 1154.

[32] A. M. Alsalme, P. V. Wiper, Y. Z. Khimyak, E. F. Kozhevnikova, I. V. Kozhevnikov, *J. Catal.* 276 (2010) 181-189.

[33] J. Happel, M. A. Hnatow, R. Mezaki, *J. Chem. Eng. Data* 16 (1971) 206-209.

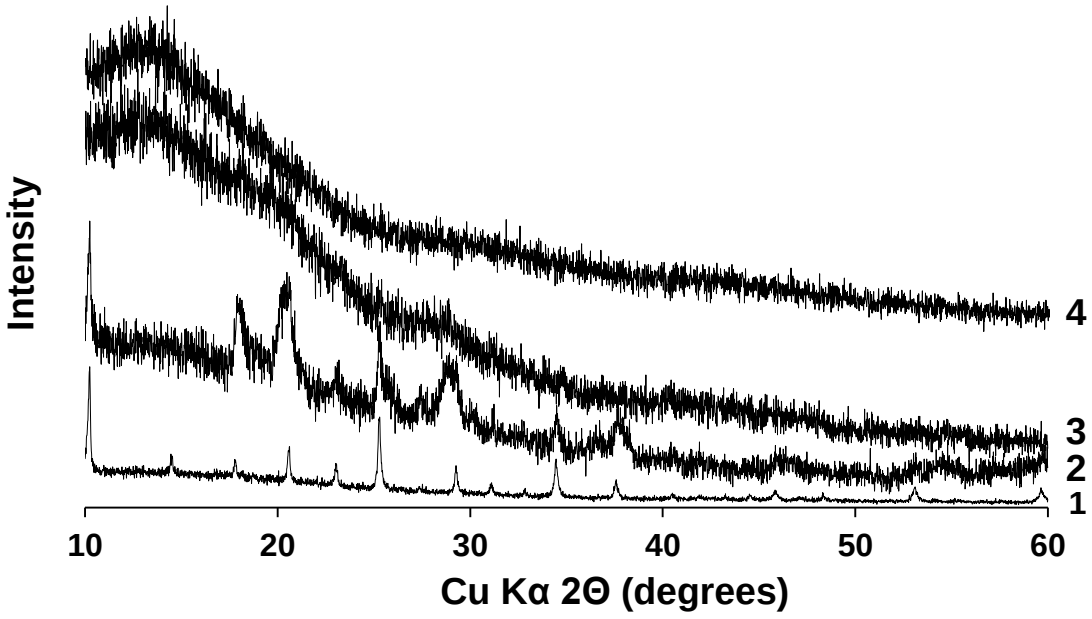

Fig. 1. XRD for bulk catalysts (air calcined at 350 ^{o}C for 2 h): (1) $H_3[PW_{12}O_{40}]$, (2) $Co_{1.5}[PW_{12}O_{40}]$, (3) $Co_{1.5}[PMo_{12}O_{40}]$ and (4) $Co_{1.5}[PMo_{12}O_{40}]$ spent catalyst.

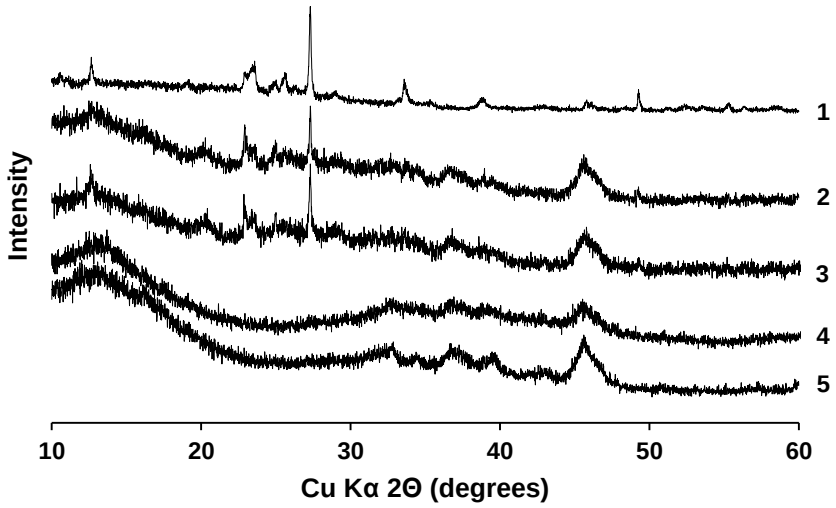

Fig. 2. XRD for supported catalysts (air calcined at 350 ^{o}C for 2 h): (1) 30%$H_3[PMo_{12}O_{40}]/SiO_2$, (2) 30%$Ni_{1.5}[PMo_{12}O_{40}]/Al_2O_3$, (3) 30%$Co_{1.5}[PMo_{12}O_{40}]/Al_2O_3$, (4) 30%$Co_{1.5}[PMo_{12}O_{40}]/Al_2O_3$ spent catalyst, (5) γ-alumina.

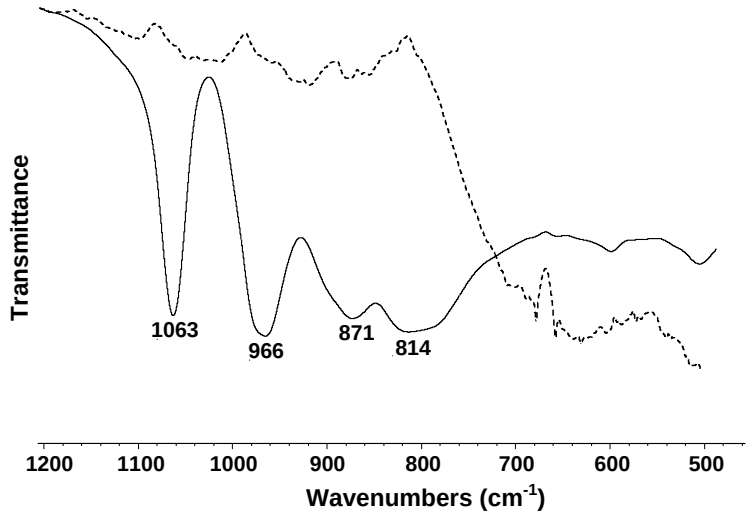

Fig. 3. DRIFT spectra of bulk $Co_{1.5}[PMo_{12}O_{40}]$ pre-catalyst (solid line) and spent catalyst (dashed line).

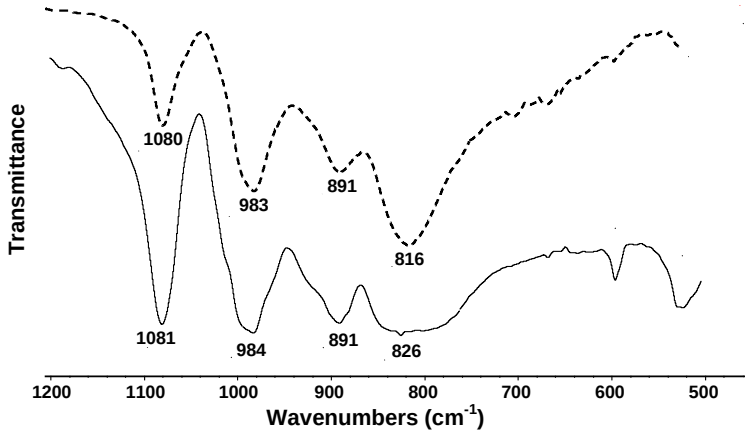

Fig. 4. DRIFT spectra of bulk $NiH[PW_{12}O_{40}]$ pre-catalyst (solid line) and spent catalyst (dashed line).

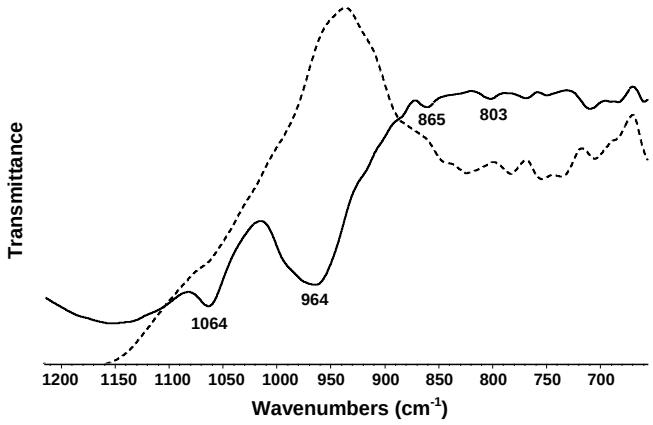

Fig. 5. DRIFT spectra of 30%$Co_{1.5}[PMo_{12}O_{40}]/Al_2O_3$ pre-catalyst (solid line) and spent catalyst (dashed line).

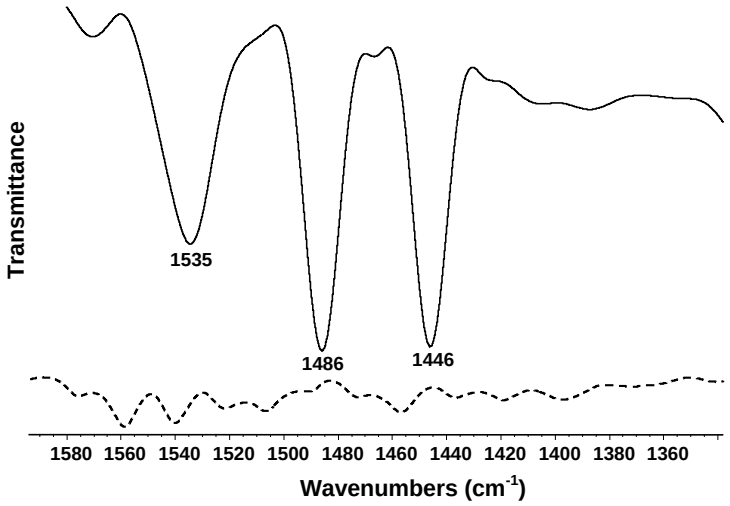

Fig. 6. DRIFT spectra of adsorbed pyridine on bulk $NiH[PMo_{12}O_{40}]$: pre-catalyst (solid line) and spent catalyst (dashed line).

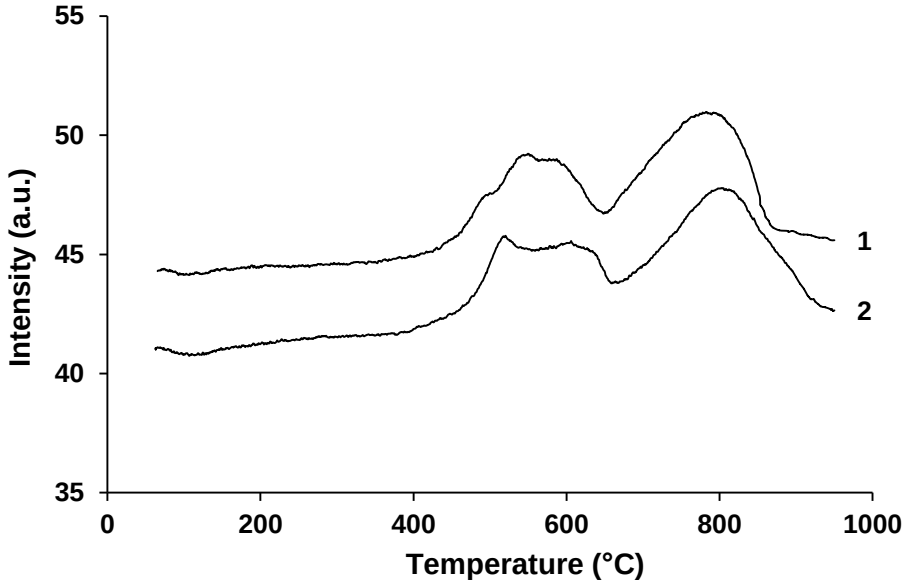

Fig. 7. H_2-TPR for pre-catalysts: (1) 30%$H_3[PMo_{12}O_{40}]/Al_2O_3$, (2) 30%$Co_{1.5}[PMo_{12}O_{40}]/Al_2O_3$.

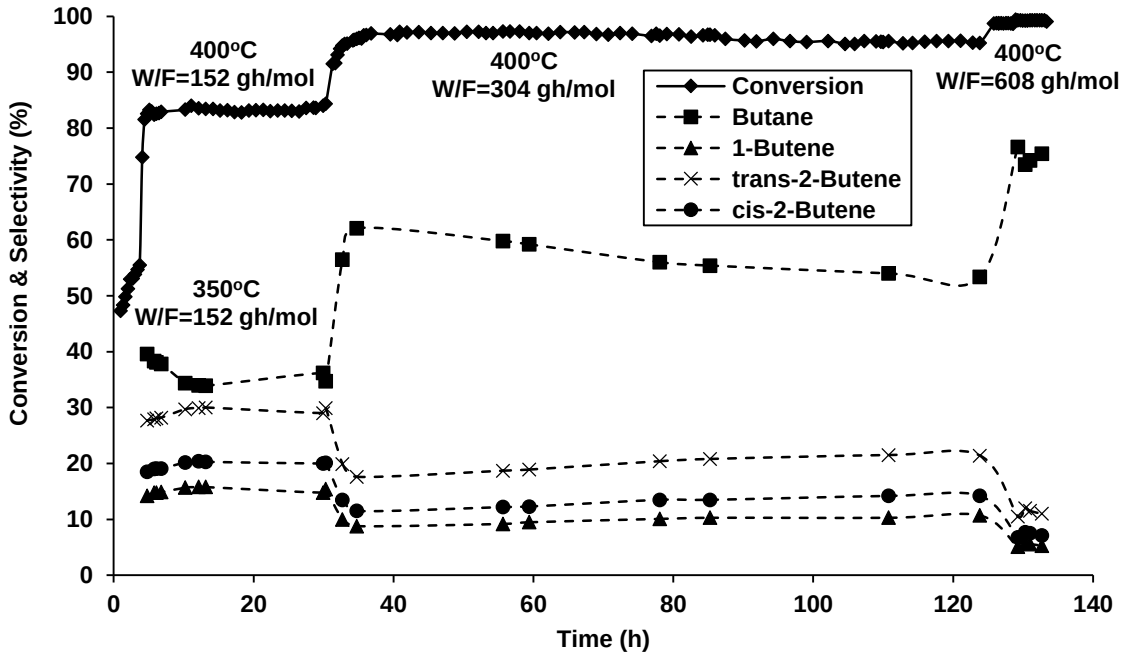

Fig. 8. Time course for HDS of thiophene over 30%$Co_{1.5}[PMo_{12}O_{40}]/Al_2O_3$ at different space times *W/F* = 152-608 g h mol^{-1} (350-400 ºC, 1 bar pressure, 2.63 kPa thiophene partial pressure in H_2 flow).

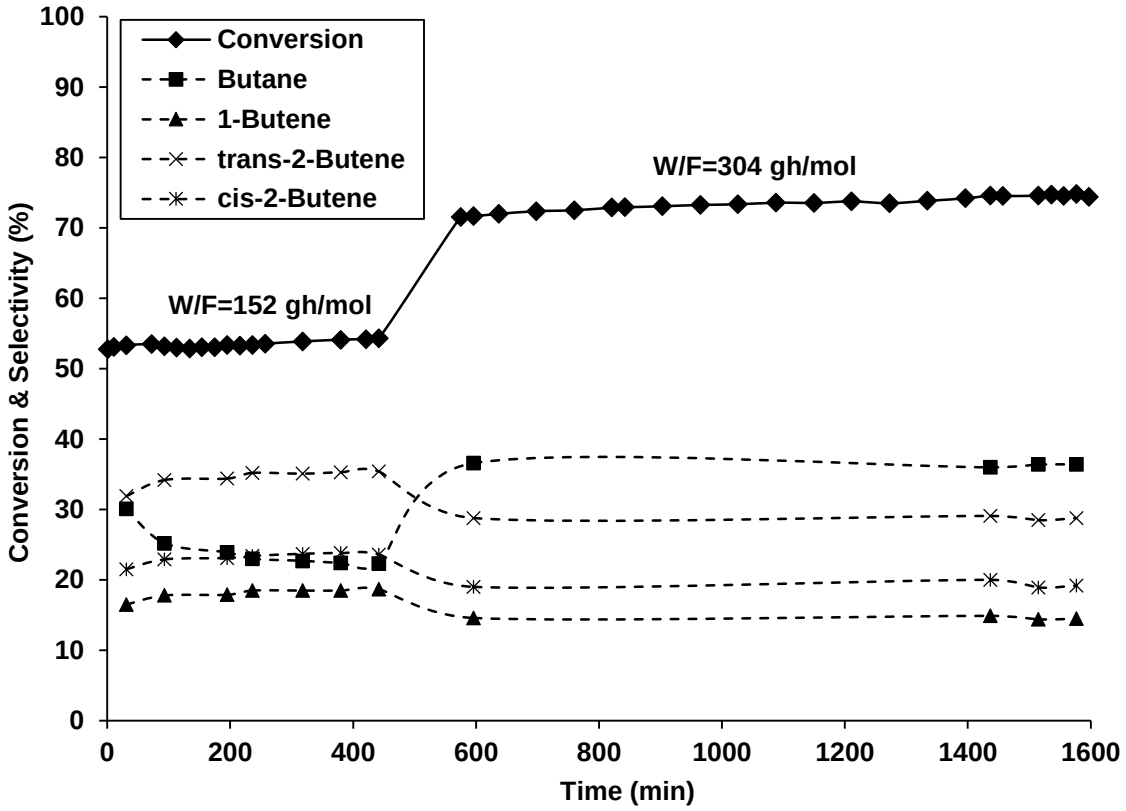

Fig. 9. Time course for HDS of thiophene over 15%$Co_{1.5}[PMo_{12}O_{40}]/Al_2O_3$ (0.20 g) at different space times *W/F* = 152-304 g h mol^{-1} (400 ^oC, 1 bar pressure, 2.63 kPa thiophene partial pressure in H_2 flow).

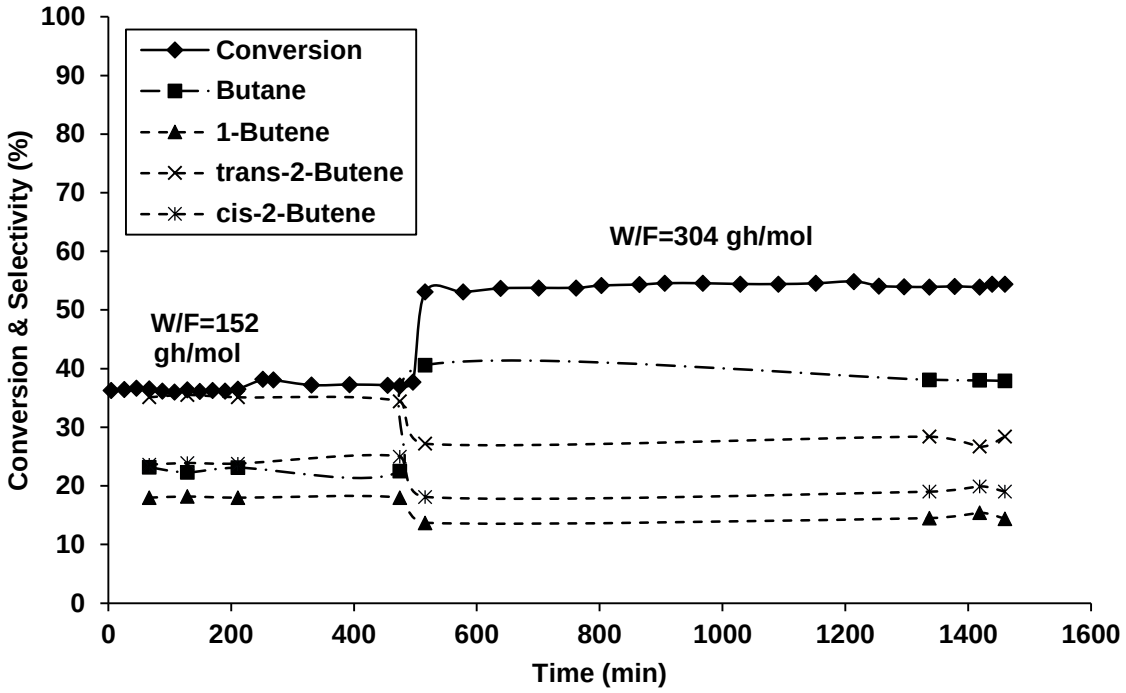

Fig. 10. Time course for HDS of thiophene over industrial CoMo catalyst ICI 41-6 (0.20 g) at different space times *W/F* = 152-304 g h mol^{-1} (400 ºC, 1 bar pressure, 2.63 kPa thiophene partial pressure in H_2 flow).

Table 1: HDS of thiophene over bulk POM catalysts.[a]

Catalyst	Conversion (%)	Selectivity (%)				
		C_4H_{10}	1-C_4H_8	trans-2-C_4H_8	cis-2-C_4H_8	others[b]
$H_3[PW_{12}O_{40}]$	0.6					
$CoH[PW_{12}O_{40}]$	0.6					
$Co_{1.5}[PW_{12}O_{40}]$	0.3					
$NiH[PW_{12}O_{40}]$	0.7					
$Ni_{1.5}[PW_{12}O_{40}]$	0.6					
$H_3[PMo_{12}O_{40}]$	2.2	21	13	14	10	42
$CoH[PMo_{12}O_{40}]$	2.0	10	10	12	8	60
$Co_{1.5}[PMo_{12}O_{40}]$[c]	1.9	14	13	13	9	51
$NiH[PMo_{12}O_{40}]$	2.6	15	15	24	15	31
$Ni_{1.5}[PMo_{12}O_{40}]$[d]	3.5	16	16	26	17	25

[a] 400 °C, 1 bar pressure, 3 h time on stream, 0.20 g catalyst amount, 2.63 kPa thiophene partial pressure in H_2 flow, 20 mL min^{-1} flow rate, W/F = 152 g h mol^{-1}, catalyst pre-sulfided for 1 h at reaction temperature. [b] C_1-C_3 hydrocarbons and isobutane.

Table 2: Hydrodesulfurisation of thiophene over non-promoted supported HPA catalysts.[a]

Catalyst[b]	Conversion (%)	Selectivity[c] (%)			
		C_4H_{10}	1-C_4H_8	trans-2-C_4H_8	cis-2-C_4H_8
$H_3[PW_{12}O_{40}]/SiO_2$	0.9				
$H_3[PW_{12}O_{40}]/TiO_2$	11	11	22	41	27
$H_3[PW_{12}O_{40}]/Al_2O_3$	4.3	5.2	21	45	28
$H_3[PMo_{12}O_{40}]/SiO_2$	19	10	19	43	28
$H_3[PMo_{12}O_{40}]/TiO_2$	29	17	20	38	25
$H_3[PMo_{12}O_{40}]/Al_2O_3$	49	25	18	35	23

[a] 400 °C, 1 bar pressure, 4 h time on stream, 0.20 g catalyst amount, 2.63 kPa thiophene partial pressure in H_2 flow, 20 mL min^{-1} flow rate, W/F = 152 g h mol^{-1}, catalyst pre-sulfided for 1 h at reaction temperature. [b] 30 wt% HPA loading. [c] Traces of C_1-C_3 hydrocarbons also formed.

Table 3: Hydrodesulfurization of thiophene over γ-Al_2O_3-supported POM catalysts promoted by Ni and Co.[a]

Catalyst[b]	Temperature (^{0}C)	Conversion (%)	Selectivity[c] (%)			
			C_4H_{10}	1-C_4H_8	trans-2-C_4H_8	cis-2-C_4H_8
$Ni^{II}H[PW_{12}O_{40}]/Al_2O_3$	350	3	20	16	38	26
	400	23	13	20	38	29
$Ni_{1.5}[PW_{12}O_{40}]/Al_2O_3$	350	4	18	14	38	30
	400	16	21	10	41	28
$CoH[PW_{12}O_{40}]/Al_2O_3$	350	1	10	23	41	26
	400	6	21	15	39	25
$Co_{1.5}[PW_{12}O_{40}]/Al_2O_3$	350	2	19	12	41	28
	400	5	21	11	40	28
$NiH[PMo_{12}O_{40}]/Al_2O_3$	350	40	27	16	34	23
	400	65	29	16	32	23
$Ni_{1.5}[PMo_{12}O_{40}]/Al_2O_3$	350	47	24	16	35	25
	400	75	40	14	27	19
$CoH[PMo_{12}O_{40}]/Al_2O_3$	350	46	33	15	31	21
	400	76	34	16	30	20
$Co_{1.5}[PMo_{12}O_{40}]/Al_2O_3$	350	52	26	17	32	25
	400	83	38	15	28	19
$Co_{1.5}[PMo_{12}O_{40}]/Al_2O_3$[d]	400	54	23	18	35	24
CoMo ICI 41-6[e]	400	37	23	18	35	24

[a] 1 bar pressure, 3 h time on stream, 0.20 g catalyst amount, 2.63 kPa thiophene partial pressure in H_2 flow, 20 mL min^{-1} flow rate, W/F = 152 g h mol^{-1}, catalyst pre-sulfided for 1 h at reaction temperature. [b] 30 wt% POM loading. [c] Traces of C_1-C_3 hydrocarbons and iso-butane also formed. [d] 15%$Co_{1.5}[PMo_{12}O_{40}]/Al_2O_3$; 8 h time on stream. [e] 8 h time on stream.